Analytica Chimica Acta 704 (2011) 133–138

Contents lists available at ScienceDirect

Analytica Chimica Acta

journal homepage: www.elsevier.com/locate/aca

Electrochemical deoxyribonucleic acid biosensor based on the self-assembly film with nanogold decorated on ionic liquid modified carbon paste electrode

Hongwei Gao[a,*], Xiaowei Qi[b], Ying Chen[c], Wei Sun[b,*]

[a] Shandong Entry-Exit Inspection and Quarantine Bureau of the People's Republic of China, Qingdao 266002, China
[b] Key Lab of Eco-chemical Engineering of Ministry of Education, College of Chemistry and Molecular Engineering, Qingdao University of Science and Technology, Qingdao 266042, China
[c] Institute of Food Safety, Chinese Academy of Inspection and Quarantine, No 3, Road Gaobeidian, Beijing, China

ARTICLE INFO

Article history:
Received 11 May 2011
Received in revised form 27 July 2011
Accepted 29 July 2011
Available online 9 August 2011

Keywords:
Carbon paste electrode
Ionic liquid
1-butylpyridinium hexafluorophosphate
Self-assemble
Electrochemical DNA biosensor
Gold nanoparticle

ABSTRACT

An electrochemical DNA biosensor was fabricated by self-assembling probe single-stranded DNA (ssDNA) with a nanogold decorated on ionic liquid modified carbon paste electrode (IL-CPE). IL-CPE was fabricated using 1-butylpyridinium hexafluorophosphate as the binder and the gold nanoparticles were electrodeposited on the surface of IL-CPE (Au/IL-CPE). Then mercaptoacetic acid was self-assembled on the Au/IL-CPE to obtain a layer of modified film, and the ssDNA probe was further covalently-linked with mercaptoacetic acid by the formation of carboxylate ester with the help of N-(3-dimethylaminopropyl)-N′-ethylcarbodiimide hydrochloride and N-hydroxysuccinimide. The hybridization reaction with the target ssDNA was monitored with methylene blue (MB) as the electrochemical indicator. Under the optimal conditions, differential pulse voltammetric responses of MB was proportional to the specific ssDNA arachis sequences in the concentration range from 1.0×10^{-11} to 1.0×10^{-6} mol L^{-1} with the detection limit as 1.5×10^{-12} mol L^{-1} (3σ). This electrochemical DNA sensor exhibited good stability and selectivity with the discrimination ability of the one-base and three-base mismatched ssDNA sequences. The polymerase chain reaction product of arachis *Arabinose operon D* gene was successfully detected by the proposed method, which indicated that the electrochemical DNA sensor designed in this paper could be further used for the detection of specific ssDNA sequence.

1. Introduction

In recent years electrochemical DNA biosensor has been widely applied due to the advantages such as high sensitivity, rapidity of response, simplicity, low cost, miniaturized and automated devices [1]. The research activities in the preparation of electrochemical biosensors for detecting DNA hybridization have dramatically increased over the past decades with the development of new materials and novel fabrication processes [2,3]. Among the preparation steps for the DNA biosensor, immobilization of biomolecular probes on a desired substrate electrode is the most important process because the performances such as sensitivity, selectivity, accuracy, reproducibility and lifetime of the sensors are significantly affected by this step. In general, the surface of the substrate and/or the terminus of DNA have to be modified for the stable immobilization of DNA probes. Various surface modification methods such as affinity binding [4], covalent attachment [5] and the use of nanomaterials [6] etc., have been demonstrated to be effective ways for the DNA immobilization. Also different detection methods including label-free or label-based approaches have been used for the hybridization reaction, which are dependent on the nature of the electrochemical signal from DNA itself or the electroactive indicators near the electrode [7,8].

Recently nanoparticles have been widely used in constructing the electrochemical DNA biosensor due to their unique characteristics such as high surface area, excellent biocompatibility, good conductivity and strong adsorption ability. Among them gold nanoparticles are the most commonly used metal nanoparticles [9,10]. The presence of gold nanoparticles on the electrode surface can not only maintain the biological activity of the immobilized biomolecules, but also promote the electron transfer rate with electrocatalytic activity simultaneously [10]. The enhancement of DNA immobilization and hybridization can also be achieved with a gold nanoparticle modified electrode [11]. Yang et al. described a DNA electrochemical biosensor with gold nanoparticle incorporated in the poly-2,6-pyridinedicarboxylic acid film modified electrode [12]. Also gold-based electrode has attracted special attentions for electrochemical DNA biosensors due to the well-defined self-assembly of thiolate at the surface of gold through Au-thiol binding [13,14]. Gu et al. [15] covalently bound the

* Corresponding authors. Fax: +86 532 84023927.
E-mail addresses: sunwei@qust.edu.cn (W. Sun), ghw75@126.com (H. Gao).

0003-2670/$ – see front matter © 2011 Elsevier B.V. All rights reserved.
doi:10.1016/j.aca.2011.07.044

single-stranded yeast DNA on 3-mercaptopropionic acid monolayer self-assembled gold electrode surface and further studied the interaction of immobilized ssDNA and dsDNA with methylene blue (MB). Sun et al. [16] covalently immobilized oligonucleotides on a self-assembled aminoethanethiol monolayer modified nanogold electrode for the target DNA sequence with daunomycin as an electroactive intercalator. DNA hybridization detection could be accomplished by electrochemical stripping of the nanogold ssDNA labels with increased sensitivity [17].

Ionic liquid modified carbon paste electrode (IL-CPE) is a new kind of working electrode prepared by using ionic liquid (IL) as a binder and a modifier. Due to the specific properties of IL such as high chemical and thermal stability, negligible vapor pressure, high ionic conductivity, wide electrochemical windows, low toxicity and the ability to dissolve a wide range of organic and inorganic compounds [18,19], IL-CPEs were demonstrated to exhibit advantages including wide electrochemical windows, inherent electrocatalytic ability and anti-fouling ability [20]. Different kinds of IL-CPEs had been fabricated and applied to the electrochemical detection of electroactive molecules. Safavi et al. [21] investigated the electrochemical oxidation of phenolic compounds on an IL-CPE, which exhibited higher stability than commonly used working electrodes. Sun et al. [22] studied the direct electrochemistry of herring sperm single-stranded DNA (ssDNA) on IL 1-butylpyridinium hexafluorophosphate ($BPPF_6$) modified CPE. IL-CPE can also been used as the substrate electrode for further modification with redox proteins or nanoparticles, which exhibited many new characteristics and potential applications [23,24].

In this paper, a novel electrochemical DNA biosensor was developed by self-assembling probe ssDNA sequence on the gold nanoparticle decorated IL-CPE with the fabrication process shown in Scheme 1. IL-CPE was prepared using $BPPF_6$ as a binder and the gold nanoparticles were electrodeposited on the IL-CPE surface by applying negative potential of −0.4 V with electrode in 5.0 mmol L^{-1} $HAuCl_4$ and 0.5 mol L^{-1} KNO_3 mixture solution. Then mercaptoacetic acid was self-assembled on the surface of Au/IL-CPE and further covalently linked with the ssDNA probe by the formation of carboxylate ester with N-hydroxysuccinimide (NHS) and N-(3-dimethylamino-propyl)-N′-ethylcarbodiimide hydrochloride (EDC). The ordering of self-assembled probe can be increased by the length of mercaptoacetic acid molecule. The hybridization reaction with the target ssDNA was monitored with the commonly used methylene blue as the electrochemical indicator. Under the optimal conditions, differential pulse voltammetric (DPV) oxidation peak currents of MB were proportional to *Arabinose operon D* gene fragments of arachis. Finally, the fabricated DNA biosensor was successful applied to the detection of polymerase chain reaction (PCR) products of *Arabinose operon D* gene, and the method showed the advantages such as the simple preparation procedure, high selectivity and broad linear range.

2. Experimental

2.1. Apparatus and chemicals

A CHI 1210A electrochemical workstation (Shanghai CH Instruments, China) was used for cyclic voltammetric and differential pulse voltammetric measurements. Electrochemical impedance spectroscopy (EIS) was performed on a CHI 750B electrochemical analyzer (Shanghai CH Instrument, China). A three-electrode system, which was composed of a modified IL-CPE as working electrode, a Pt wire as auxiliary electrode and a saturated calomel electrode (SCE) as reference electrode, was used throughout. Scanning electron microscopy (SEM) was obtained by a JSM-6700F scanning electron microscope (Japan Electron Company, Japan).

1-Butylpyridinium hexafluorophosphate ($BPPF_6$, >99%, Lanzhou Greenchem. ILS, LICP, CAS, China), graphite powder (average particle size 30 μm, Shanghai Colloid Chemical Co. Ltd. China), chloroauric acid ($HAuCl_4$, Shanghai Chemical Plant, China), mercaptoacetic acid (MAA, Tianjin Yuanhang Chemical Co. Ltd., China), N-(3-dimethyl-amino-propyl)-N′-ethylcarbodiimide hydrochloride (EDC, Sigma, USA), N-hydroxy-succinimide (NHS, Shanghai Medpep Co. Ltd., China), Sodium dodecyl sulfate (SDS, Shanghai Hengda Fine Chemical Co., Ltd., China) and methylene blue (MB, Shanghai Chemicals Plant, China) were used as received. All the solutions were prepared with doubly distilled water and other chemicals used were of analytical grade.

The 22-base oligonucleotides probe (probe ssDNA), target complementary sequence DNA (target ssDNA), one-base mismatched ssDNA, three-base mismatched ssDNA and noncomplementary sequence DNA (ncDNA) were synthesized by Shanghai Sangon Biological Engineering Tech. Co. Ltd. (China), which were related to *Arabinose operon D* gene sequence of arachis. Their base sequences were as below:

Probe ssDNA: 5′-NH_2-GTC CAA GTC GCA ACG CTG TGG T-3′,
Target ssDNA: 5′-ACC ACA GCG TTG CGA CTT GGA C-3′,
One-base mismatched ssDNA: 5′-ACT ACA GCG TTG CGA CTT GGA C-3′,
Three-base mismatched ssDNA: 5′-ACT ACA GCG TTA CGA CTT GTA C-3′,
ncDNA: 5′-TCA CGC AGA CGT TTT GCC GGT A-3′.

The DNA sample for polymerase chain reaction amplification was extracted from arachis oil. The PCR reaction was performed on an Eppendorf Mastercycler Gradient PCR system using oligonucleotide primers for *Arabinose operon D* gene of arachis with the following sequences:

Primer F: 5′-GCA ACA GGA GCA ACA GTT CAA G-3′
Primer R: 5′-CGC TGT GGT GCC CTA AGG-3′

2.2. Fabrication of MAA/Au/IL-CPE

Ionic liquid modified carbon paste electrode was fabricated with the following procedure. Initially, 3.0 g of graphite powder, 1.0 g of $BPPF_6$ and 0.5 g liquid paraffin were mixed thoroughly in a mortar and further heated at 80 °C to form a homogeneous carbon paste. A portion of the carbon paste was filled into one end of a glass tube (Ø = 4 mm) and a copper wire was inserted through the opposite end to establish an electrical contact. Prior to use, a mirror-like surface was obtained by polishing the electrode on a weighing paper. Gold nanoparticle modified IL-CPE (Au/IL-CPE) was prepared based on a reported procedure [25]. In general, gold nanoparticles were electrodeposited by applying −0.4 V for 300 s to a freshly prepared IL-CPE placed in 5.0 mmol L^{-1} $HAuCl_4$ and 0.5 mol L^{-1} KNO_3. Then, the Au/IL-CPE was rinsed with doubly distilled water and dried in air for further modification.

MAA/Au/IL-CPE was prepared by immersing the Au/IL-CPE in a 5.0 mL of 10.0 mol L^{-1} aqueous MAA solution for 24 h to form a self-assembled monolayer. Then, the electrode was rinsed thoroughly with doubly distilled water to remove physically adsorbed MAA. The electrode was dried in air at room temperature to obtain a modified electrode denoted as MAA/Au/IL-CPE.

2.3. Fabrication of electrochemical DNA biosensor

Immobilization of probe ssDNA sequence was achieved by immersing MAA/Au/IL-CPE in 5.0 mL of 50.0 mmol L^{-1} phosphate buffered saline (PBS, pH 7.0) containing 5.0 mmol L^{-1} EDC and 8.0 mmol L^{-1} NHS for 30 min at room temperature to activate the

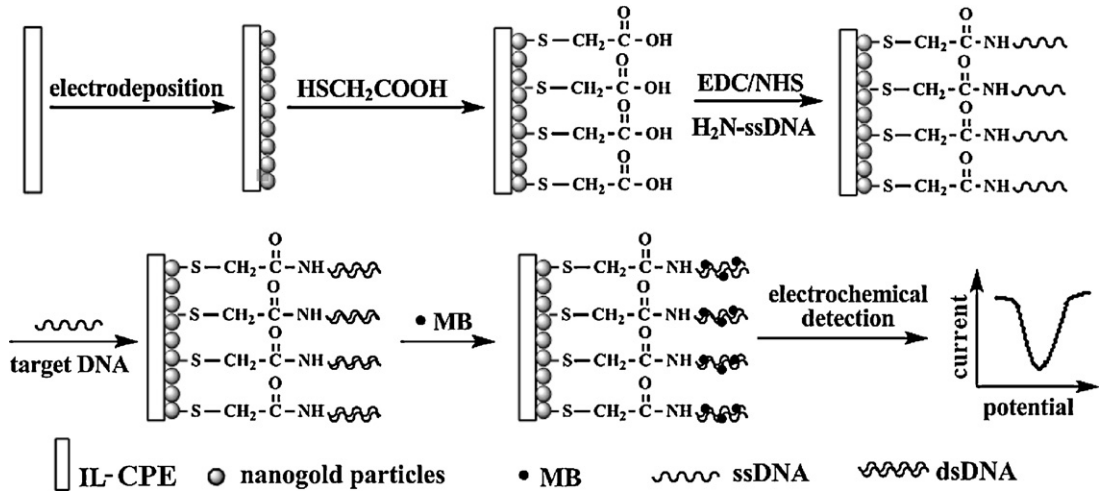

Scheme 1. A schematic representation of the electrochemical DNA biosensor.

electrode interface. Then 10 μL 50.0 mmol L^{-1} PBS (pH 7.0) containing 1.0×10^{-6} mol L^{-1} probe ssDNA sequence was applied to the electrode surface. After being dried in air at room temperature, the electrode surface was washed with 0.5% SDS solution and PBS for 3 times successively, to remove unabsorbed probe ssDNA on the electrode surface. Due to the covalent interaction between the carboxyl group of MAA and the amino group of ssDNA, a stable probe ssDNA film was formed on the electrode surface and this is further denoted as ssDNA/MAA/Au/IL-CPE.

The hybridization assay was carried out by immersing probe ssDNA/MAA/Au/IL-CPE in 50.0 mmol L^{-1} PBS containing different concentrations of target ssDNA for 40 min at 40 °C with stirring. Then the electrode was washed with 0.5% SDS solution and PBS for 3 times successively to remove the unhybridized target ssDNA, and this hybridized electrode is denoted as dsDNA/MAA/Au/IL-CPE.

2.4. Electrochemical detection

After hybridization the modified electrode was immersed into 5.0 mL of 2.0×10^{-5} mol L^{-1} MB solution for 10 min, which could accumulate MB molecules on the hybrid interface, then the electrode was washed with 0.5% SDS solution and PBS for 3 times. The electrochemical response of MB was measured by differential pulse voltammetry in a 50.0 mmol L^{-1} Tris–HCl buffer solution (pH 7.0) with a pulse amplitude as 0.001 V, a pulse width as 0.05 s and a pulse period as 0.2 s.

2.5. Polymerase chain reaction procedure

Amplification of *Arabinose operon D* gene fragments was carried out in a final volume of 25 μL in 0.2 mL tube containing 200.0 nmol L^{-1} each primer of *Arabinose operon D* gene sequence primer F and primer R, 10× reaction buffer B (Promega, Wisconsin USA), 2.0 mmol L^{-1} $MgCl_2$, 200.0 nmol L^{-1} each of dATP, dCTP, dGTP and dTTP, 1.5 units of Taq DNA polymerase (Promega, Wisconsin USA), 1.0 μL DNA template purified from samples. During the PCR procedure, DNA was initially denatured at 94 °C for 30 s. PCR conditions were optimized as follows: 35 cycles of amplification (94 °C for 30 s, 56 °C for 30 s, 72 °C for 30 s) and final extension at 72 °C for 5 min. 6 μL each of the PCR products were analyzed by electrophoresis separation (5 V cm^{-1}, 40 min) on a 2% agarose gel containing 0.5 μg mL^{-1} of ethidium bromide in 1× TAE buffer (40.0 mmol L^{-1} Tris, 1.0 mmol L^{-1} EDTA, 40.0 mmol L^{-1} acetate, pH 8.0). The PCR products of *Arabinose operon D* gene were kept at 4 °C before use.

3. Results and discussion

3.1. SEM image of the modified electrodes

SEM was used to study and compare the morphology of different modified electrodes with the results showed in Fig. 1. On the IL-CPE a uniform surface was observed (Fig. 1A). Due to the high viscosity and good conductivity, IL can disperse the graphite powder in the paste, which is in agreement with the previous reported result [26]. After electrodeposition of gold nanoparticles on the IL-CPE surface, the interface appeared with dendritic gold structures (Fig. 1B). The nanostructure was symmetrical to the bone-axis, and many small nanoparticles appeared and interconnected linearly on the IL-CPE surface. The results indicated successful deposition of gold nanoparticles on the IL-CPE with an increased surface area and a three-dimensional dendritic structure [27], which was further used for the formation of a self-assembled film.

3.2. Electrochemical behaviors of modified electrodes

Cyclic voltammograms of different modified electrodes in a 1.0 mmol L^{-1} $[Fe(CN)_6]^{3-}$ solution were recorded and shown in Fig. 2A. A quasi-reversible redox behavior of $[Fe(CN)_6]^{3-/4-}$ was observed on IL-CPE with peak-to-peak separation (ΔE_p) of 110 mV at the scan rate of 100 mV s^{-1} (curve a), indicating the good conductivity of IL-CPE and the result was attributed to the high ionic conductivity of IL in the carbon paste. While on Au/IL-CPE the redox peak currents increased with the ΔE_p decreased to 77 mV (curve b), indicating the presence of high conductive gold nanoparticles on the electrode surface. After the self-assembled of MAA, the electrochemical responses on MAA/Au/IL-CPE were decreased (curve c), which was due to the presence of negatively charged MAA monolayer on the electrode surface hindered the electron transfer of negatively charged $[Fe(CN)_6]^{3-/4-}$. The electrode responses were further decreased on the ssDNA/MAA/Au/IL-CPE (curve d) and dsDNA/MAA/Au/IL-CPE (curve e), indicating the presence of DNA film further retarded the electron transfer rate. According to the Randles–Sevcik equation [28]:

$I_{pc} = (2.69 \times 10^5) n^{3/2} A D^{1/2} C^* v^{1/2}$, where I_{pc} is the reduction peak current (A), n is the electron transfer number, A is the electroactive surface area (cm^2), D is the diffusion coefficient of $K_3[Fe(CN)_6]$ in the solution (cm^2 s^{-1}), C^* is the concentration of $K_3[Fe(CN)_6]$ (mol cm^{-3}) and v is the scan rate (V s^{-1}), the electroactive surface area of different electrodes can be calculated. By exploring the redox peak current with the scan rate, the average electroactive

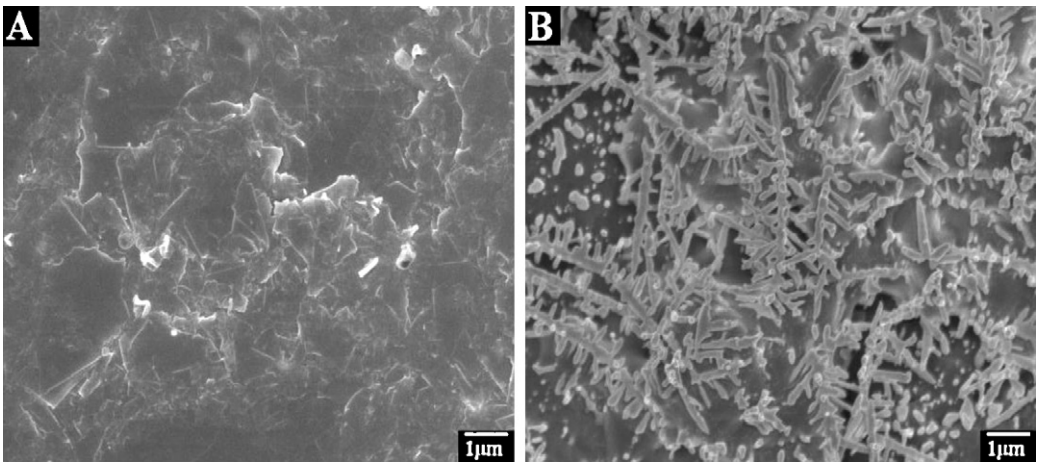

Fig. 1. SEM images of IL-CPE (A) and gold nanoparticles decorated IL-CPE.

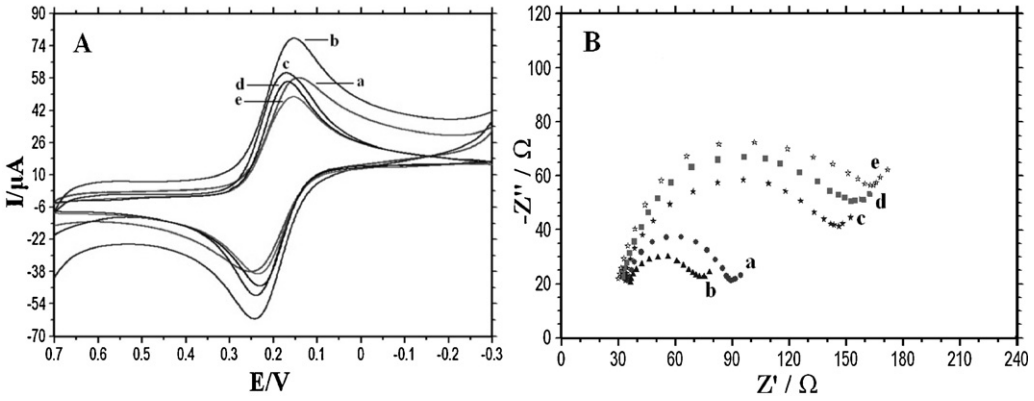

Fig. 2. (A) Cyclic voltammograms of different modified electrodes in 1.0 mmol L^{-1} $K_3[Fe(CN)_6]$ and 0.5 mol L^{-1} KCl with scan rate as 100 mV s^{-1}; (B) electrochemical impedance spectra of different modified electrodes in 1.0 mmol L^{-1} $[Fe(CN)_6]^{3-/4-}$ containing 0.1 mol L^{-1} KCl with the frequency sweep from 10^4 to 1.0 Hz. Electrodes used from a to e were IL-CPE, Au/IL-CPE, MAA/Au/IL-CPE, ssDNA/MAA/Au/IL-CPE and dsDNA/MAA/Au/IL-CPE, respectively.

area of IL-CPE and Au/IL-CPE were calculated as 0.163 and 0.241 cm^2, respectively. The results also indicated the presence of gold nanoparticles greatly improved the effective area.

EIS can be used to probe the interfacial electron transfer resistance (R_{et}) on the modified electrodes, and the semicircle portion observed at high frequencies in the Nyquist diagrams corresponds to the electron transfer limiting process. The Nyquist diagrams of different modified electrodes in 1.0 mmol L^{-1} $[Fe(CN)_6]^{3-/4-}$ solution were recorded with the frequencies swept from 10^4 to 1.0 Hz and the results were shown in Fig. 2B. The interfacial electron transfer resistance (R_{et}), which derived from the semicircle diameter of impedance spectra, was equaled to 56.6 Ω for IL-CPE (curve a). After the electrodeposition of gold nanoparticles, the R_{et} value decreased to 40.9 Ω (curve b). By immobilizing gold nanoparticles on the electrode surface, the increase conductivity and surface area would be expected to encourage additional electron transfer between electrode and electrolyte. On the MAA/Au/IL-CPE and ssDNA/MAA/Au/IL-CPE the Ret values increased to 137.9 Ω (curve c) and 151.3 Ω (curve d), respectively, indicating the presence of MAA and ssDNA could hinder the electron transfer of ferricyanide on the electrode surface. On the dsDNA/MAA/Au/IL-CPE, the R_{et} value was further increased to 157.7 Ω (curve e), suggesting that DNA hybridization led to the increased resistance for electron transfer at the electrode surface, and this was a further proof of the hybridization reaction between probe ssDNA and target ssDNA. The EIS results were also in good agreement with cyclic voltammetric responses of $[Fe(CN)_6]^{3-/4-}$ on the modified electrode.

3.3. Performances of modified electrodes

MB is a phenothiazine dye that is a commonly used indicator in the development of electrochemical DNA biosensor [8,15,29–31]. MB can exhibit different interaction models with ssDNA and dsDNA, which depends on both the DNA sequences and the experimental conditions such as ion strength, MB concentration and buffer pH. Ozsoz et al. [31] reported the specific interaction of MB with guanine bases in DNA sequence. MB also can interact with phosphate framework of ssDNA by electrostatic binding, while the electrostatic effect and intercalation with the major or minor grooves of dsDNA helix are coexisted, which results in the higher affinity of dsDNA with MB and can be used to distinguish the dsDNA and ssDNA [15,32]. Fig. 3A showed the differential pulse voltammograms of MB at different electrodes in 50.0 mmol L^{-1} Tris–HCl buffer solution (pH 7.0). On the IL-CPE an oxidation peak of MB appeared at −0.326 V (curve a), which was attributed to the electrode reaction of phenothiazine group. On the Au/IL-CPE the oxidation peak current increased (curve c), indicating the higher conductivity of the electrode surface due to the presence of gold nanoparticles. While on MAA/Au/IL-CPE the response decreased a little (curve b) because the MAA self-assembled monolayer on the gold nanoparticles immobilized electrode hindered the electron transfer of MB on the electrode. On the ssDNA/MAA/Au/IL-CPE the response was increased (curve d), indicating that ssDNA was successfully immobilized on the MAA monolayer. MB can interact with ssDNA by electrostatic attraction and accumulate on the

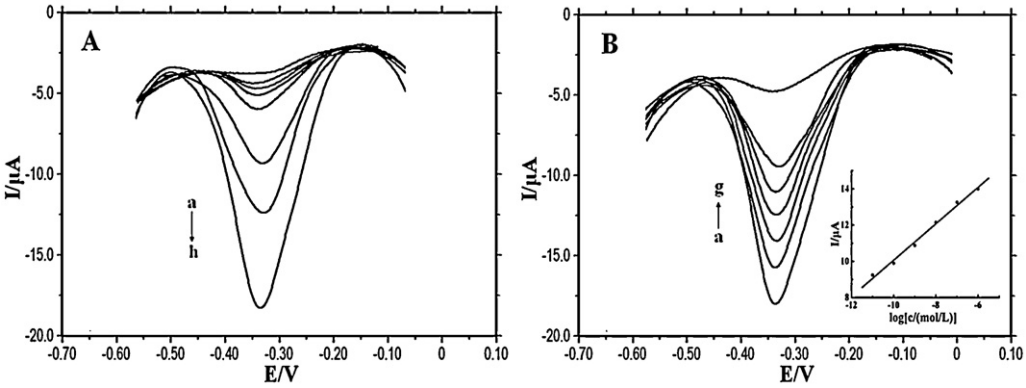

Fig. 3. (A) Differential pulse voltammograms of MB at the IL-CPE(a), MAA/Au/IL-CPE (b), Au/IL-CPE(c), ssDNA/MAA/Au/IL-CPE (d) and after hybridization with the non-complementary sequence (e), three-base mismatched sequence (f), one-base mismatched sequence (g), the complementary ssDNA sequence (h); (B) differential pulse votlammegrams of MB on ssDNA/MAA/Au/IL-CPE after hybridization with different concentrations of target ssDNA sequence. Concentrations of target ssDNA sequence from a to g were 1.0×10^{-6}, 1.0×10^{-7}, 1.0×10^{-8}, 1.0×10^{-9}, 1.0×10^{-10}, 1.0×10^{-11} and 0 mol L^{-1}, respectively. Insert: plots of I versus logarithm of target ssDNA concentration.

electrode surface. The electrochemical response was further increased on the dsDNA/MAA/Au/IL-CPE (curve h). After hybridization with the complementary ssDNA sequence the dsDNA molecules were formed on the electrode surface and more MB molecules were expected to intercalate in the dsDNA structure, leading to a large electrochemical response.

Fig. 3A also shows the selectivity of the electrochemical DNA biosensor that was hybridized with different ssDNA sequences related to target ssDNA sequence, such as the noncomplementary sequence (curve e), three-base mismatched sequence (curve f), one-base mismatched sequence (curve g) and the complementary DNA sequence (curve h). The highest MB oxidation signal was obtained at the electrode hybridization with complementary ssDNA sequence (curve h), indicating that the largest attachment of MB occurred at this electrode because of the strong affinity of MB with the formed dsDNA. The peak current of MB was very small after the ssDNA probe was reacted with the noncomplementary sequence (curve e), indicating that the hybridization reaction was not achieved in the solution. The little increase of the peak current was due to the non-specific adsorption of ssDNA on the electrode surface. After the ssDNA probe was hybridized with the one-base mismatched sequence (curve g) and three-base mismatched sequence (curve f), the peak current increased was much smaller than that obtained from the result of the complementary ssDNA sequence. Also the one-base mismatched sequence and the three-base mismatched sequence could be recognized via the different changes of the peak current of MB. The results demonstrated that this DNA biosensor displayed higher selectivity for the hybridization detection.

The sensitivity of this electrochemical DNA biosensor was examined using the immobilized ssDNA probe to hybridize with different concentrations of the *Arabinose operon D* gene target ssDNA sequence. With the increase of the target ssDNA concentration in the solution the oxidation peak current of MB was increased gradually with the typical differential pulse voltammograms shown in Fig. 3B, indicating more hybridization reaction occurred on the electrode surface. The change in MB anodic peak current before and after hybridization was linear with the logarithmic value of the *Arabinose operon D* gene target ssDNA sequence concentration in the range from 1.0×10^{-11} to 1.0×10^{-6} mol L^{-1} with the linear regression equation as $I/\mu A = 1.005 \log[c/(\text{mol L}^{-1})] + 20.11$ ($n = 6$, $\gamma = 0.996$). The relative standard deviation (RSD) of peak current for the 7 repeated detections of 1.0×10^{-7} mol L^{-1} target sequence was 2.7%, indicating the good reproducibility. A detection limit of the *Arabinose operon D* gene target sequence was estimated to be 1.54×10^{-12} mol L^{-1} (3σ) (where σ is the RSD of the blank solution, $n = 11$).

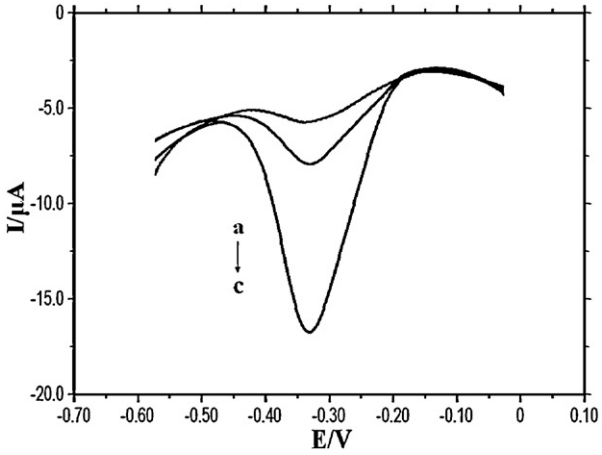

Fig. 4. Differential pulse votlammograms of MB on MAA/Au/IL-CPE (a), ssDNA/MAA/Au/IL-CPE (b) and ssDNA/MAA/Au/IL-CPE hybridized with the PCR product of *Arabinose operon D* gene sample (c).

The stability of ssDNA/MAA/Au/IL-CPE was further investigated by hybridizing with the target sequence and the results indicated that the ssDNA sequence could be tightly immobilized on the electrode surface due to the covalently reaction. After 14 days storage of the modified electrode at 4 °C, 98.1% of the initial sensitivity remained, indicating this modified electrode was a stable platform as electrochemical DNA biosensor.

3.4. Specific sequence detection of PCR product of Arabinose operon D gene sequence

The hybridization detection of the PCR amplified real-life sample of *Arabinose operon D* gene of arachis, which was extracted from arachis oil, was further performed by the developed method. The *Arabinose operon D* gene amplified samples were diluted with 50.0 mmol L^{-1} PBS (pH 7.0) and denatured by heating it in a boiling water bath for 10 min, and then frozen in an ice bath for 2 min to obtain the ssDNA solution. The ssDNA/MAA/Au/IL-CPE was immersed in the solution of the denatured PCR amplification product from *Arabinose operon D* gene sample. After hybridization the electrochemical detection was conducted by the experimental procedure described in Section 2.4 and the results are shown in Fig. 4. The MB signal at the MAA/Au/IL-CPE (curve a) was 58.0% smaller than that at the *Arabinose operon D* gene ssDNA probe electrode (curve b), indicating that the presence of ssDNA on the electrode surface could adsorb small amounts of MB molecules by

electrostatic attraction with the oxidation peak current appeared. This peak current could be used as the background value and the current differences before and after the hybridization was used for the qualitative detection. The MB oxidation peak current was increased to 12.3 μA after the hybridization with PCR product of *Arabinose operon D* real sample (curve c), indicating the successful accomplishment of the hybridization reaction with dsDNA formed on the electrode surface. This significant difference of the MB signals between the *Arabinose operon D* gene probe ssDNA electrode and at the hybridized dsDNA electrode confirmed that this DNA biosensor could effectively detect the PCR product of *Arabinose operon D* gene sample that extracted from arachis oil.

4. Conclusions

In this paper, an improved DNA electrochemical sensor was developed by self-assembling a probe ssDNA on a nanogold decorated IL-CPE and further applied to the detection of the PCR product of *Arabinose operon D* gene sample extracted from arachis oil. The surface of the modified electrodes was characterized by different methods including SEM, cyclic voltammetry and electrochemical impedance spectroscopy. The mentioned method provided a simple strategy for the preparation of gold nanoparticles modified IL-CPE and the gold nanoparticles deposited could be easily controlled to some extent by choosing different solution concentrations, deposition times and deposition potentials. Due to the presence of gold nanoparticles on the IL-CPE surface, a stable mercaptoacetic acid self-assembled film was formed, which was then used for the covalently link to the probe ssDNA sequence. This DNA electrochemical sensor was applied to the detection of *Arabinose operon D* gene sequence of arachis with a dynamic concentration range from 1.0×10^{-11} to 1.0×10^{-6} mol L^{-1} and the detection limit of 1.5×10^{-12} mol L^{-1} (3σ). The PCR product of *Arabinose operon D* gene sample extracted from arachis oil was also detected satisfactorily.

Acknowledgements

We acknowledge the financial support provided by the project of Chinese Academy of Inspection and Quarantine (Jianke2009jk033), National Department Public Benefit Research Foundation (201110015), 11th Five Years Key Programs for Science and the Shandong Province Natural Science Foundation (ZR2009BL017).

References

[1] J. Wang, Anal. Chim. Acta 500 (2003) 247–257.
[2] E. Katz, I. Willner, J. Wang, Electroanalysis 16 (2004) 19–44.
[3] L. Liu, Q.S. Huo, Appl. Phys. Lett. 87 (2005) 133902–133904.
[4] J.W. Park, H.-Y. Lee, J.M. Kim, R. Yamasaki, T. Kanno, H. Tanaka, H. Tanaka, T. Kawai, J. Biosci. Bioeng. 97 (2004) 29–32.
[5] E.G. Hvastkovs, D.A. Buttry, Langmuir 25 (2009) 3839–3844.
[6] L.D. Tran, B.H. Nguyen, H.V. Nguyen, H.V. Tran, Mater. Sci. Eng. C 31 (2011) 477–485.
[7] Y.W. Hu, T. Yang, X.X. Wang, K. Jiao, Chem. Eur. J. 16 (2010) 1992–1999.
[8] W. Sun, P. Qin, H.W. Gao, G.C. Li, K. Jiao, Biosens. Bioelectron. 6 (2010) 1264–1270.
[9] M.T. Castañeda, S. Alegret, A. MerkoÅi, Electroanalysis 19 (2007) 743–753.
[10] J.M. Pingarrón, P. Yáñez-Sedeño, A. González-Cortés, Electrochim. Acta 53 (2008) 5848–5866.
[11] T. García, E. Casero, M. Revenga-Parra, J. Martín-Benito, F. Pariente, L. Vázquez, E. Lorenzo, Biosens. Bioelectron. 24 (2008) 184–190.
[12] J. Yang, T. Yang, Y.Y. Feng, K. Jiao, Anal. Biochem. 365 (2007) 24–30.
[13] S. Rho, D. Jahng, J.H. Limb, J. Choi, J.H. Chang, S.C. Lee, K.J. Kimb, Biosens. Bioelectron. 23 (2008) 852–856.
[14] C.Z. Li, Y. Liu, J.H.T. Luong, Anal. Chem. 77 (2005) 478–485.
[15] J.Y. Gu, X.J. Lu, H.X. Ju, Electroanalysis 14 (2002) 949–954.
[16] X. Sun, P. He, S. Liu, J. Ye, Y. Fang, Talanta 47 (1998) 487–495.
[17] J. Wang, D.K. Xu, A.N. Kawde, R. Polsky, Anal. Chem. 73 (2001) 5576–5581.
[18] J.F. Liu, G.B. Jiang, J.Å. Jönsson, Trends Anal. Chem. 24 (2005) 20–27.
[19] S. Pandey, Anal. Chim. Acta 556 (2006) 38–45.
[20] D. Wei, A. Ivaska, Anal. Chim. Acta 607 (2008) 126–135.
[21] A. Safavi, N. Maleki, F. Tajabadi, Analyst 132 (2007) 54–58.
[22] W. Sun, Y.Z. Li, M.X. Yang, S.F. Liu, K. Jiao, Electrochem. Commun. 10 (2008) 298–301.
[23] W. Sun, X.Q. Li, P. Qin, K. Jiao, J. Phys. Chem. C 113 (2009) 11294–11300.
[24] W. Sun, Y.Z. Li, K. Jiao, Electrochim. Acta 45 (2009) 4105–4110.
[25] W. Sun, P. Qin, R.J. Zhao, K. Jiao, Talanta 80 (2010) 2177–2181.
[26] W. Sun, R.F. Gao, K. Jiao, J. Phys. Chem. B 111 (2007) 4560–4567.
[27] X. Xu, J. Jia, X. Yang, S. Dong, Langmuir 26 (2010) 7627–7631.
[28] A.J. Bard, L.R. Faulkner, Electrochemical Methods, 2nd ed., Wiley, New York, 2001.
[29] A. Erdem, K. Kerman, B. Meric, M. Ozsoz, Electroanalysis 13 (2001) 219–223.
[30] B. Meric, K. Kerman, D. Ozkan, P. Kara, S. Erensoy, U.S. Akarca, M. Mascini, M. Ozsoz, Talanta 56 (2002) 837–846.
[31] W.R. Yang, M. Ozsoz, D.B. Hibbert, J.J. Gooding, Electroanalysis 14 (2002) 1299–1302.
[32] S.O. Kelley, J.K. Batron, Bioconjugate Chem. 8 (1997) 31–37.